INDONESIAN JOURNAL ON GEOSCIENCE
Geological Agency
Ministry of Energy and Mineral Resources

Journal homepage: http://ijog.geologi.esdm.go.id
ISSN 2355-9314, e-ISSN 2355-9306

Micron to Nano Au Particles Incorporation in Different Stages of Pyrite, in Bau, Sarawak, Malaysia

Vijay Anand Sundarrajan[1], Carolyn Nicole Marjon[1], and Baba Musta[2]

[1]Department of Applied Sciences (Applied Geology), Curtin University, CDT 250, Miri, Sarawak-98009, Malaysia.
[2]Faculty of Science and Natural Resources, Universiti Malaysia Sabah, Kota Kinabalu, Sabah-88400, Malaysia.

Corresponding author:
Manuscript received: March, 01, 2024; revised: Octoberber, 05, 2024; approved: March, 17, 2025; available online: April, 23, 2025

Abstract - In eastern Malaysia, Bau is the significant sediment hosted gold deposit (SHG), and Sarawak Province was the main gold (Au) producer in East Malaysia. The annual production rate was approximately 40–50 metric tons of Au (high grade). The Bau mining is located 40 km SW of Kuching City, Sarawak. For the present study, around twenty-five samples were collected in the Au mineralized zones of Bau areas. The polished thin sections were prepared for mineral chemistry and fluid petrography analyses. The samples were studied through transmission microscope, Electron Probe Micro-Analyzer (EPMA), and fluid inclusion studies. From ore petrography, four stages of pyrite were classified. The first generation of pyrite is the early stage of diagenetic pyrite (Py1), Py2 is subeuhedral pyrite, Py3 is zoned pyrite, and Py4 is post-diagenetic pyrite. The mineral chemistry of different stages of pyrite was measured through EPMA. However, it is worth noting that the concentrations of these trace elements in pyrite have decreased pre-diagenetic and post-diagenetic stages. The precipitation of Au in the main stages of pyrite was mainly controlled by pyrite structure, fluid ligands, and the temperature of crystallization.

Keywords: Bau gold, pyrite, sediment hosted Au deposit, fluid inclusion, EPMA

How to cite this article:
Sundarrajan, V.A., Marjon, C.N., and Musta, B., 2025. Micron to Nano Au Particles Incorporation in Different Stages of Pyrite, in Bau, Sarawak, Malaysia. *Indonesian Journal on Geoscience*, 12 (1), p.89-103. DOI: 10.17014/ijog.12.1.89-103

Introduction

Background

Au plays a critical role as a mineral resource globally, as its occurrences aid to the economic status of the country (Goldfarb, 2021). It is a commodity which naturally forms within various deposits and geodynamic settings (Wilford, 1955; Wolfenden 1965; Hon, 1981; Sillitoe and Bonham, 1990; Kirwin and Royle, 2018; Katz *et al*., 2021; Goldfarb, 2021). In eastern Malaysia, Bau is one of the significant sediments hosted Au deposits and main producers in Sarawak. The Bau Au mining is located 40 km SW of Kuching City, Sarawak, eastern Malaysia. In the year of 1830 - 1860, the Chinese people mined sporadically before the British colonial activities commenced in the early 1900s (Kirwin and Royle, 2018). Bukit Young Sdn. Bhd. took over the area in the late 1990s (Kirwin and Royle, 2018). Currently, Besra Gold (previously known as Olympus Pacific Minerals) manages the Bau Project through its partially (92.06

%) owned subsidiary North Kalimantan Gold. The Au occurs along the mineralized trend belt of Bau regions, hosted in thinly bedded silty dolomite or limestones, and cut across by steep dipping faults (Wilford, 1955; Wolfenden, 1965; Hon, 1981; Sillitoe and Bonham, 1990; Macdonald, 2007; Kirwin and Royle, 2018). The production rate was approximately 40 - 50 metric tons of Au per year.

For the past three decades, a research on the Au within sulphides has been carried out by several researchers globally (Cook and Chryssoulis, 1990; Butler and Rickard, 2000; Muntean *et al*., 2011; Zhu *et al*., 2011; Kirwin and Royle, 2018; Large and Maslennikov, 2020). It occurs in microscopic-nano size represents lattice bound Au (Cook and Chryssoulis, 1990; Pour *et al*., 2014). Several forms of Au occuring in Bau deposit, which comprises carbonate-replacement ore bodies, hydrothermal veins, Au-bearing calcic skarns were reported (Percival *et al*., 1990; Pour *et al*., 2014). The primary mineralization took place between 12 - 10 Ma. After the ceaseless Au exploration over Bau has resulted in depleted reserves, high-grade Au production declines, driving producers to divert their focus to low-grade Au deposits (Large and Maslennikov, 2020). The deposits predominantly composed of invisible gold with size ranging from submicron to nanoparticles are commonly observed within pyrite and arsenopyrite (Farrand, 1970; Cabri *et al*., 1989; Morishita *et al*., 2018; Large and Maslennikov, 2020). Despite that, due to the submicroscopic size and its mineralogical location, there are a confined number of studies on "invisible" gold. Till now, there is no similar research was conducted in the Bau gold deposits, Kuching. The present study is to classify the different stages of pyrite, textures, the amount of Au, and trace element incorporation in multiple stages of pyrite, and to understand the origin of the gold and the precipitation mechanism.

Geological Settings

In eastern Malaysia, Lupar Fault Zone strikes WNW 50 km to the north of Bau, and delineates northern and southern Kalimantan Island (Mustard, 1997; Yao, 1999) (Figure 1). Northern Kalimantan represents the Cenozoic accretionary wedge with turbiditic sediments of the Rajang Group (Upper Cretaceous to Eocene) in the south and Crocker Formation flysch (Oligocene to Lower Miocene) in the northern region (Moss and Chambers, 1999; Yao, 1999; Lambiase *et al*., 2008). The Lupar and Belaga Formations constitute the Rajang Group in Sarawak (Galin *et al*., 2017; Ahmed *et al*., 2020). The Kuching Zone is divided among five tectono-stratigraphic zones of Kalimantan, separated from the Sibu Zone by the Lupar Line Fault (Wang *et al*., 2016) (Figure 1). The subduction occurred in Late Triassic forming the lavas and andesitic pyroclastic of the Serian Volcanics (Mustard, 1997). Volcanic rocks (*i.e.* tuffs, andesite flows, amygdaloidal lavas, and pyroclastic breccias) drilled from the Tai Parit deposits adjudicated Serian Volcanics form the oldest deposit of Bau (Schuh, 1993; Mustard, 1997). It was stated to correlate to the deposits in Serian which are 70 km away from Bau (by road).

Early Jurassic Jagoi granodiorites comprising medium-grained, nonporphyritic, hornblende-bearing granitoids (Schuh, 1993), forms in the trench suction in fore-arc basin (Schuh, 1993).

By the Mid-Jurassic era up till Early Cretaceous, the subduction ended, and a period of uplift and erosion begun forming the shelf and slope deposits of the Bau limestone and Pedawan Formation (Tan, 1986). Bau Limestone Formation occurs as karstic hills with caves covered by alluvium (Tate, 1991; Mustard, 1997; Hutchison, 2005), typically massive grey, and consists of carboniferous fossiliferous (micrite) limestone with micritic matrix (Hutchison, 2005; Mustard, 1997). The limestone in this formation comprises mainly calcite (98 %) with dolomite (2 %) (Schuh, 1993). Bau Limestone Formation extensively forms beyond the border into NW Kalimantan (Tate, 1991). In the Late Cretaceous, rock uplifting in Bau produced major folds in the region before the deposition of Kayan sandstone above Pedawan Formation occurred in the Early Tertiary (Wolfenden, 1965; Muller 1968). Frequently rocks, seen in the Bau District, are from the Pedawan

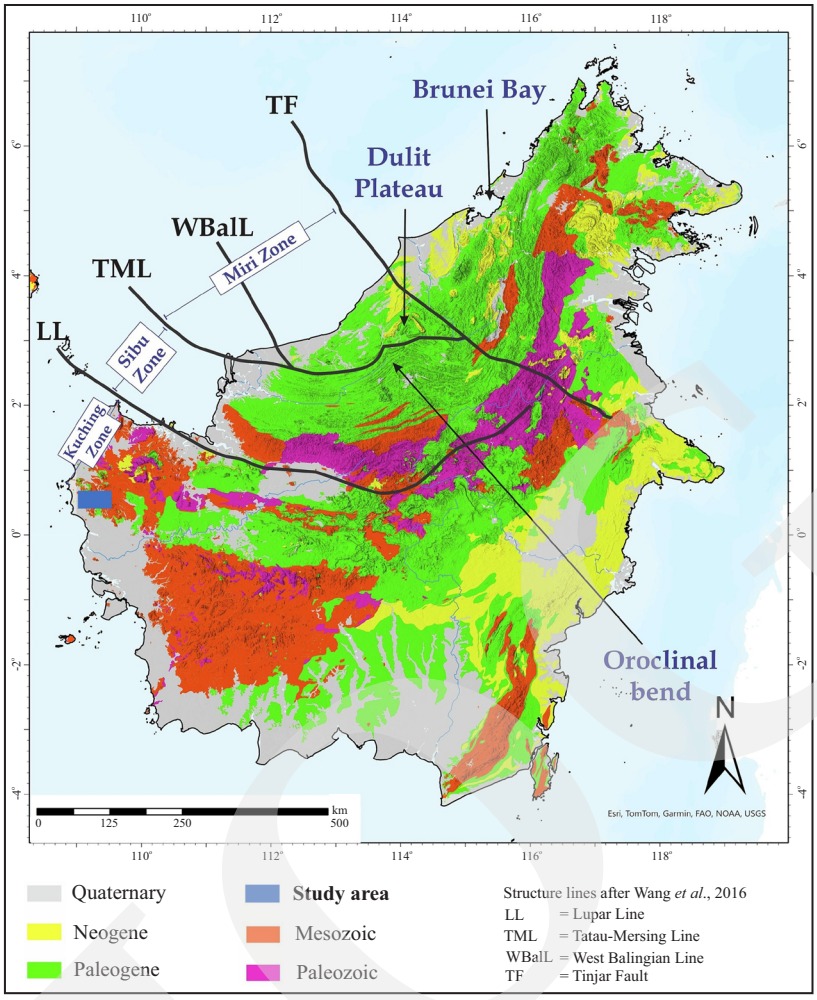

Figure 1. Regional geological map of the Kalimantan Island, highlighting black lines and major stratigraphic zones (Modified after Syafiq *et al.*, 2024).

Formation. The Pedawan Formation posseses two distinct tectonic layers: the upper is turbidite (> 90 %) layer of euxinic shales and sandstones, the latter is oceanic sediment (< 10 %). Epithermal Au-As-(Sb), disseminated Au, and low-temperature Hg-As discernible in this formation (Schuh, 1993).

The mineral deposits of the Bau gold field show district-scale zoning over a 10 km strike. The mafic magmatism transport the mineralized fluids from porphyry copper core and associated skarns (Gunung Ropih and Gunung Juala) to proximal carbonate replacement deposits (Taiton and Sarabau) and more distal sediment-hosted deposits (Pejiru, Jugan, and Bukit Sarin) (Percival *et al.*, 1990; Schuh, 1993; Percival and Hofstra, 2002; Pour *et al.*, 2014). Metals observed in Bau District include the porphyry Cu-Mo-Au, skarn Cu-Au, carbonate replacement/skarn Zn-Pb-Ag-Au, and sediment hosted Au-Ag-Sb (Royle, 2015). The sediment-hosted gold deposits emplaced between deep-seated faults and other structures (Berger *et al.*, 2014; Kirwin and Royle, 2018). The majority of NNE faults and conjugate set NW transform faults transpired along with seafloor spreading (Eocene and Early Miocene) in the bay area (Mustard, 1997).

Research Methods

Field Sampling

A detailed fieldtrip was conducted in several locations of the Bau District. The samples were collected in the following locations: Jugan

Hill (1.4488°N, 110.204°E), Gunong Paku (Sin Seng Ann Quarry) (1.4278°N, 110.182°E), Jalan Kuching (1.4218°N, 110.173°E), Niang-Niang Temple (1.4074°N, 110.152°E), and Jalan Pejiru (1.3279°N, 110.069°E).

Thin Section

Twenty-five thin sections were prepared for petrography analysis. The mineral assemblages were included to determine the sulphide and other ore minerals. The petrographic features were observed in Nikon Eclipse LV 100N Pol Microscope and Nikon Camera in the mineralogy laboratory of Curtin University, Miri, Malaysia.

Electron Probe Micro-Analyzer (EPMA) Analysis

After a thorough assessment through petrographic analysis of different stages of pyrite, two mineralized samples were selected for electron probe micro-analyzer (EPMA) for Au and trace element analyses. The analytical conditions for instrument were 20 kV accelerating voltage and 100nA beam current. The count times for Fe and S were 20 s, and for other elements were 80 s. The standards of the Fe-S (FeS_2), As, Au, Co, Ni, and Cu were used for analyses. Well-polished thin sections were prepared for EPMA analysis. Around twenty spots were chosen for different stages of pyrites. The samples were analyzed in Indian Institute of Technology, Bombay, India (Instrument Model. EPMA-1720 HT).

Results

Field Observations

In the SW Kuching towards Bau Town, sulphide rich shales (STT) (Jugan Hill) and limestone (**SSA**) samples were collected over Gunong Paku (Sin Seng Ann Quarry) (Figure 2). The host rocks in Jugan Hill intensively folded and overturned with obvious shearing on the interbedded shales and siltstones of the Pedawan Formation. In the dark grey to black carbonaceous shale ore body (Figures 3a - b), however, excursion was only carried out in the Sin Seng Ann Quarry region with the right authorization and supervision. Light grey lime-

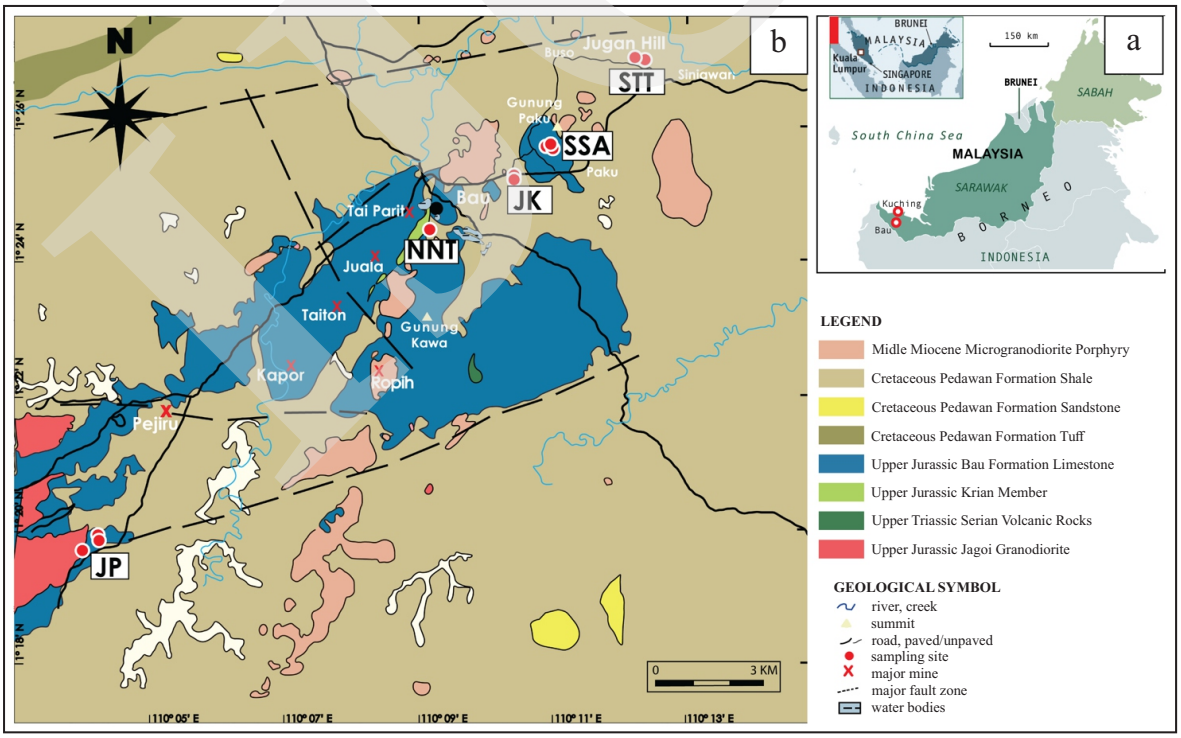

Figure 2. (a) Map of eastern Malaysia and location of Bau and Kuching Districts. (b) Location map and the geological layer of Bau District. Symbols in white boxes indicate sampling sites (Modified after Kirwin and Royle, 2018).

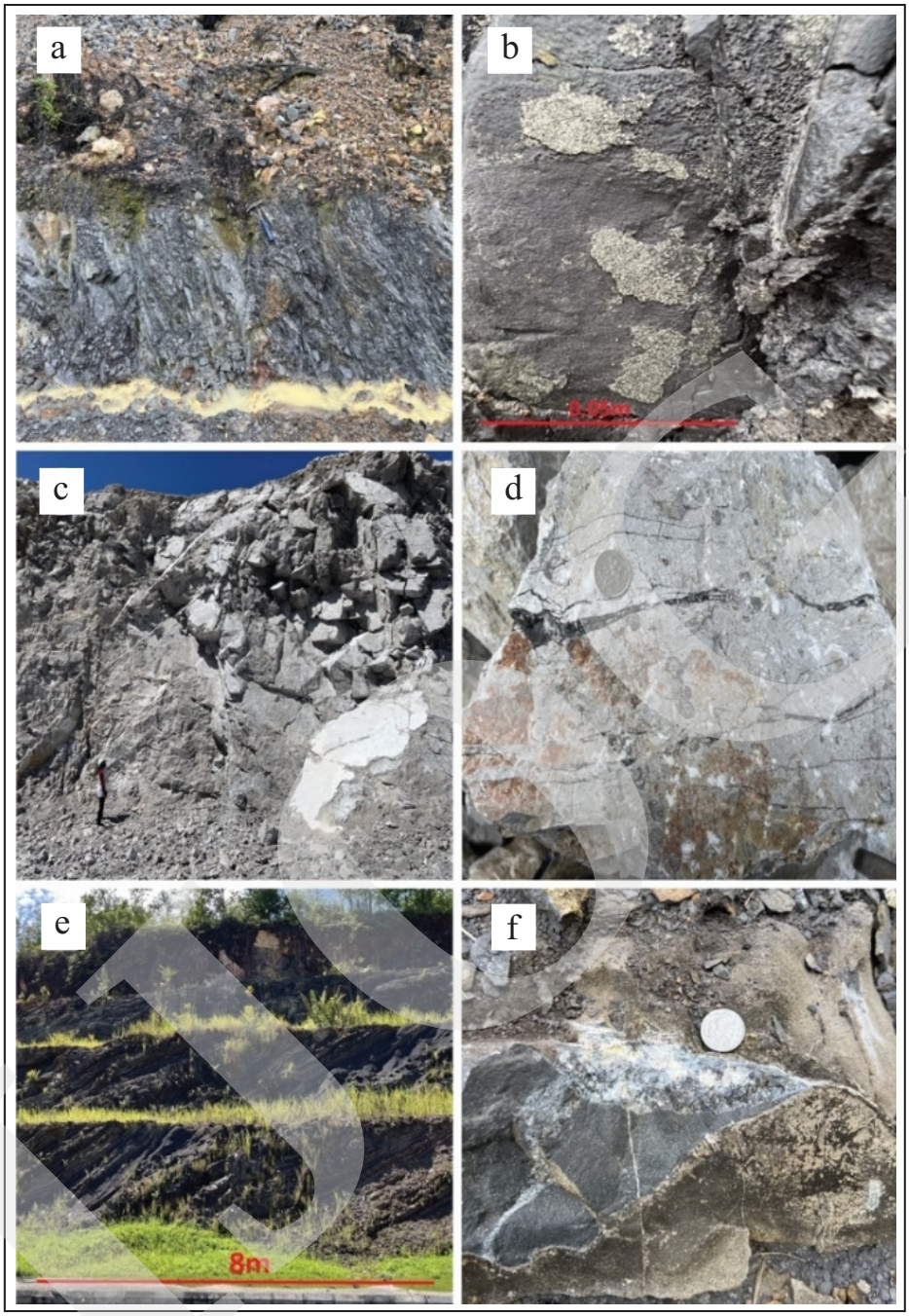

Figure 3. Field photographs demonstrating the geological and mineralization features of the Bau gold deposit, eastern Malaysia. (a) Siliceous shale and carbonaceous shale bedding in Jugan Hill with strike and dip reading of 220°/44° SE. (b) Very fine-grained cubic pyrite on carbonaceous shale of the Pedawan Formation (Jugan Hill). (c) Limestone bedding (Bau Limestone Formation) observed in Sin Seng Ann Quarry with strike and dip reading of 140/50 NE. (d) Fossiliferous calcite veins limestone boulder on the ground of Sin Seng Ann Quarry. (e-f) Road side outcrop of interbedded sandstone and siltstone (Pedawan Formation) in Jalan Kuching and Jalan Pejiru, Bau, Kuching.

stones of the Bau Limestone Formation (Figure 3c) with numerous calcite veins and carbonate grains (Figure 3d) formed the quarry. Two groups of calcite veins typically hosted in the carbonate rock are bed-parallel veins and strike veins. The next sampling location is a road side outcrop exposed in Jalan Kuching next to a shop lot (Figure 3e) which displays the Pedawan Formation beds of shales, siltstone, thinly bedded sandstone, and limestone with strike and dip of 134°/40° NE. The fine-grained

disseminated pyrite, chalcopyrite (Figures 4, 5b - 5c), pyrite aggregate (Figure 4c, 5c), and acicular arsenopyrite (Figures 5e - 5f) can be observed. Located further SW of Jugan Hill, Gunong Paku is heavily mined for its limestones. These quarries are run by three different companies which include SSF Quarry, Sin Seng Ann Quarry, and Marup Quarry. Two major faults were observed: normal faulting in the centre of the outcrop and thrust fault in the south of the outcrop with 096°/60° NE and 048°/68° N, respectively. Calcite veins (062°/34° NE) are also discernible in this region, predominantly on limestone and carbonaceous shale. Limestone and shale with veins samples collected from this region was labeled as JK. Passing the road to Bau Town, right after Niang-Niang Temple, on an unattended land in Jalan Taman Indah, there is a pile of dark grey limestone with vein networks gravels. No beds or outcrop was observed in this area. However, samples were still collected from this region and labeled as NNT. The last site is situated by the road of Jalan Pejiru (further towards SSW), next to a local residence.

Mineralized Limestone

Pyrite generally comprises < 1 % volume of the host rock as dispersed fine to very fine grains in early mineralization stages. Pyrite hosted in

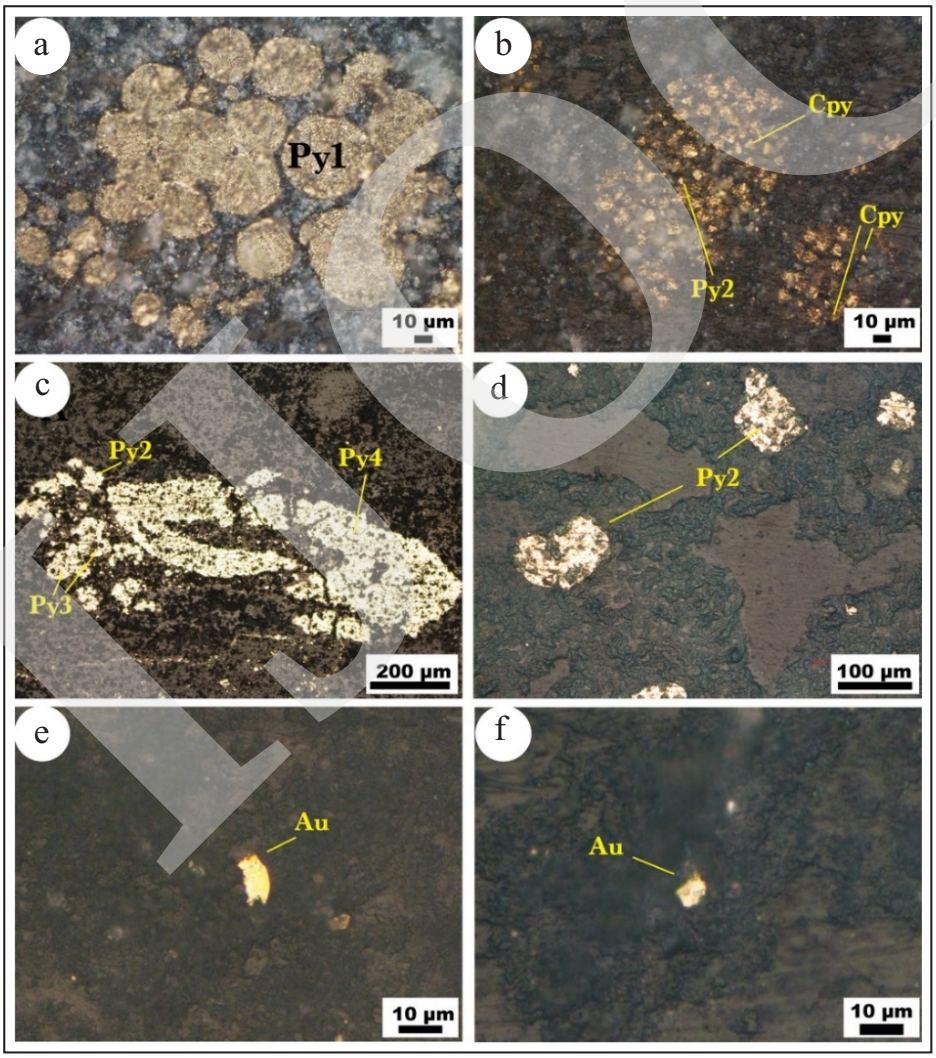

Figure 4. Reflected light photomicrographs demonstrating pyrite paragenesis of Bau Formation, Sin Seng Ann Quarry, and Jalan Kuching. (a) Poly-framboidal pyrite, Py1; (b) Subhedral to euhedral pyrite alongside of chalcopyrite (Py2 and Cpy1); (c) Fracture filling and aggregate of pyrite; (d) Disseminated subhedral to euhedral pyrite (Py2) (e-f) Very fine-grained of gold in limestone. Abbreviations; Py1 (Pyrite1); Py2 (Pyrite2), Py3 (Pyrite3), Py4 (Pyrite4), CPy1 (Chalcopyrite1).

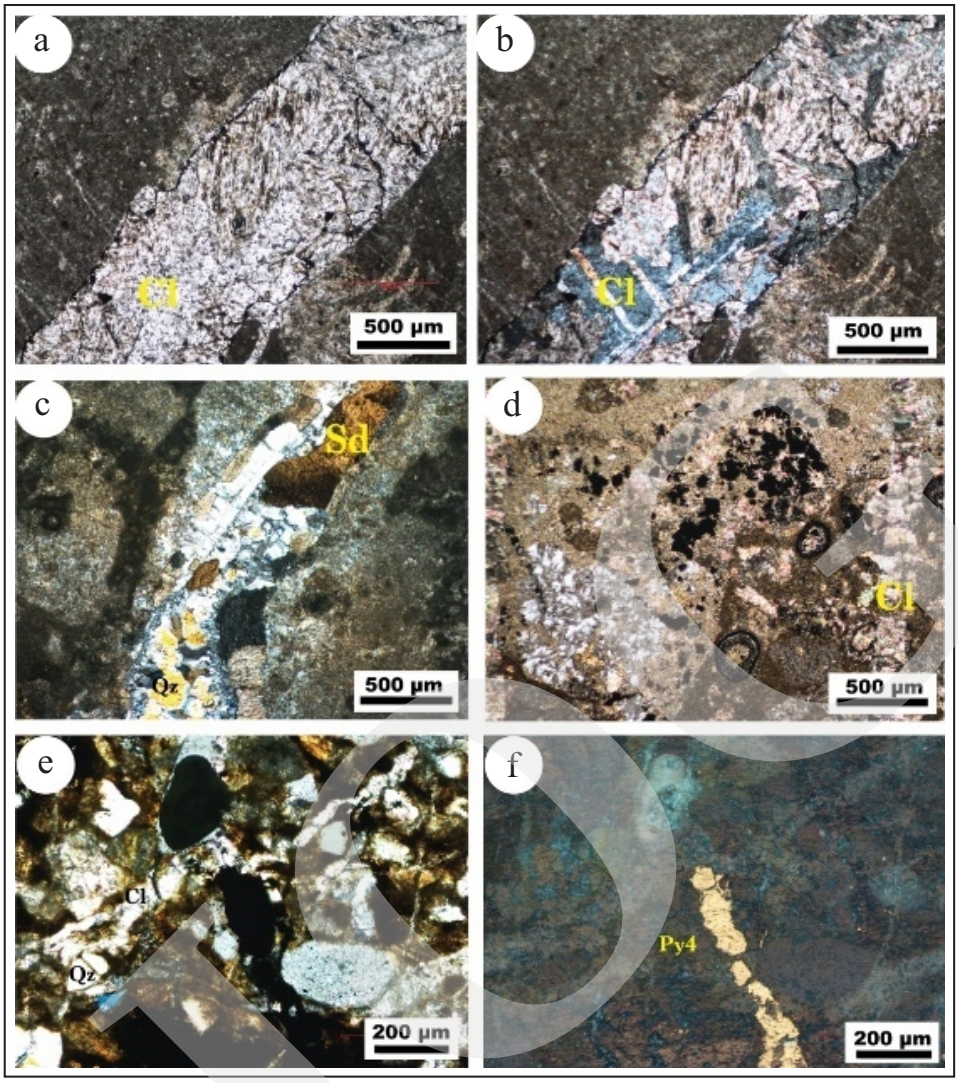

Figure 5. Polarized light and reflected light photomicrographs display the textural features and mineral assemblages from the sediment-hosted gold deposit Bau, Kuching, Sarawak; (a-b) Polarized light of calcite (Cal) vein and initial crystallization of dolomite (JPP); (c) Crossed polarized light image of quartz veins siderite precipitating within (JK1); (d) Fine grained subhedral to euhedral pyrite disseminated and replacing ooids structure in limestone samples from Jalan Kuching (JK5(2); (e-f) Crossed polarized light and reflected light of pyrite precipitating within fractures in Qz + Cl veins of sample JK3.

the limestones mainly consists of all the pyrite varieties. Py1 and Py2 occur sporadically across the samples from Sin Seng Ann Quarry with size ranging from 5 µm to 100 µm. However, limestone samples collected from Jalan Kuching composed of Py1, Py2, and Py4 (Figure 5).

Chalcopyrite is relatively abundant in the limestone samples from Jalan Kuching (Figure 5). It occurs as irregular to triangular shapes amongst euhedral pyrite grouped together forming spherical to subspherical shaped clusters.

Very fine-grained gold is observed under the reflected light microscopy in the limestone (carbonate) samples (Bau and Pedawan contact zones) (Figure 5). The gold is encompassed by the mix of dolomite spar cement and finer dolomite. These subhedral gold grains are 12.5µm and 0.75µm in size, respectively.

Ore Mineralogy

Through the reflected light microscopes, sulphides are characterized according to their types, and stages are summarized in Table 1.

Carbonates formed predominantly throughout Bau comprise limestones, dolomites, and calcite. The limestones are generally micritic, veinitic,

Table 1. Classification of Sulphide Minerals and their Textures, Au Deposit

Sulphide Classification	Colour	Textures	Host Rock	Occurrence Style
Py1	Light yellow	Framboidal, poly-framboidal	Limestone, Shale	Fine-grained, clustered along with chalcopyrite
Py2		Subhedral-Euhedral, fine-grained		Disseminations, Co-exist with chalcopyrite
Py3		Hydrothermal Rim, Zoning		Disseminations, Overgrows chalcopyrite or Py2,
Py4		Cluster or aggregate of subhedral to euhedral pyrite		Fracture filling, veinlets and disseminations
Aspy1	Silver white	Rhombic, acicular, fine-grained	Shale	Disseminations, co-exists with Py1, Py2
Aspy2		Spiculate, Actinomorphic, fine-grained	Shale	Disseminations, co-exists with Py1, Py2, Apy2
Cpy1	Yellow	Fine-grained subhedral to euhedral, triangle	Limestone	Disseminations, co-exist with pyrite
Cpy2		fracture filling	Shale	Aggregates

with bioclasts such as echinoids, ooids, red algae, foraminifera, and reef. Most of the veins found in the limestone formation consist of calcite veins with varying size. Under the microscope, some calcite veins are accompanied by dolomite (dolomite grains have nucleated around the calcite) (Figure 5). Calcite veins formed in Jalan Kuching often developed alongside of quartz-calcite veins.

Mineralized Shale

Pyrite is dominant in the carbonaceous and mineralized shale (Figures 6 and 7). Py2, Py3, and Py4 are commonly observed and co-existing with chalcopyrite and arsenopyrite. Early Py1 was predominantly found disseminated in the euxinic shale of Jugan Hill as very fine grains.

Chalcopyrite is easily distinguished in the carbonaceous shale from the Jugan Hill as it is distinctively yellow in colour with low reflectivity compared to the light-yellow pyrite. In the bedded-laminar pyritic shale (STT1), chalcopyrite occurs as fracture fillings (Cpy2), and coincides with Py2, Py3, and Py4 as shown in Figures 5b and 5c.

Arsenopyrite is often observed disseminated in the reworked carbonaceous shale deposit of Pedawan Formation in Jugan Hill. Arsenopyrite grains developed as acicular-prismatic with stellar and drusoid intergrowths (Figures 5e and f). The crystals size is approximately ≥ 257 μm.

Silicate minerals include quartz, biotite, muscovite mica, hornblende, and a variety of clay minerals. The quartz grains are generally enclosed with clay minerals, lithic fragments, fracture filling pyrite, and calcite veins in quartz-calcite vein. Figure 5c shows the inclusions of siderite and the growth of siderite in quartz veins.

EPMA Results

The EPMA analysis of Au and trace element concentrations in different stages of pyrite for two samples from Jugan Hill and Jalan Kuching are summarized in Table 2. The first generation of Py1 which demonstrates low concentrations of Au (45 - 70 ppm), low Co/Ni ratio (< 1 ppm), and low As content (450 - 520 ppm). The second stage of pyrite (Py2) is frequently observed throughout the Bau Au deposit which is displayed in reflected light photomicrographs (Figures 4 - 6). These pyrites are the main ore stage as Au concentrations (390 - 282 ppm) which are highest in this stage. Arsenic concentrations (650 - 570 ppm) and Co/Ni ratio (2.6 - 1.8) are accordant to the high Au content. This third generation of pyrite (Py3) is common in the carbonaceous shale deposit of Jugan Hill as overgrowth on subhedral to euhedral pyrite (Py2). Py3 contains high concentration of Au (220 - 175 ppm). However, it is worth noting that the concentrations of these trace elements in

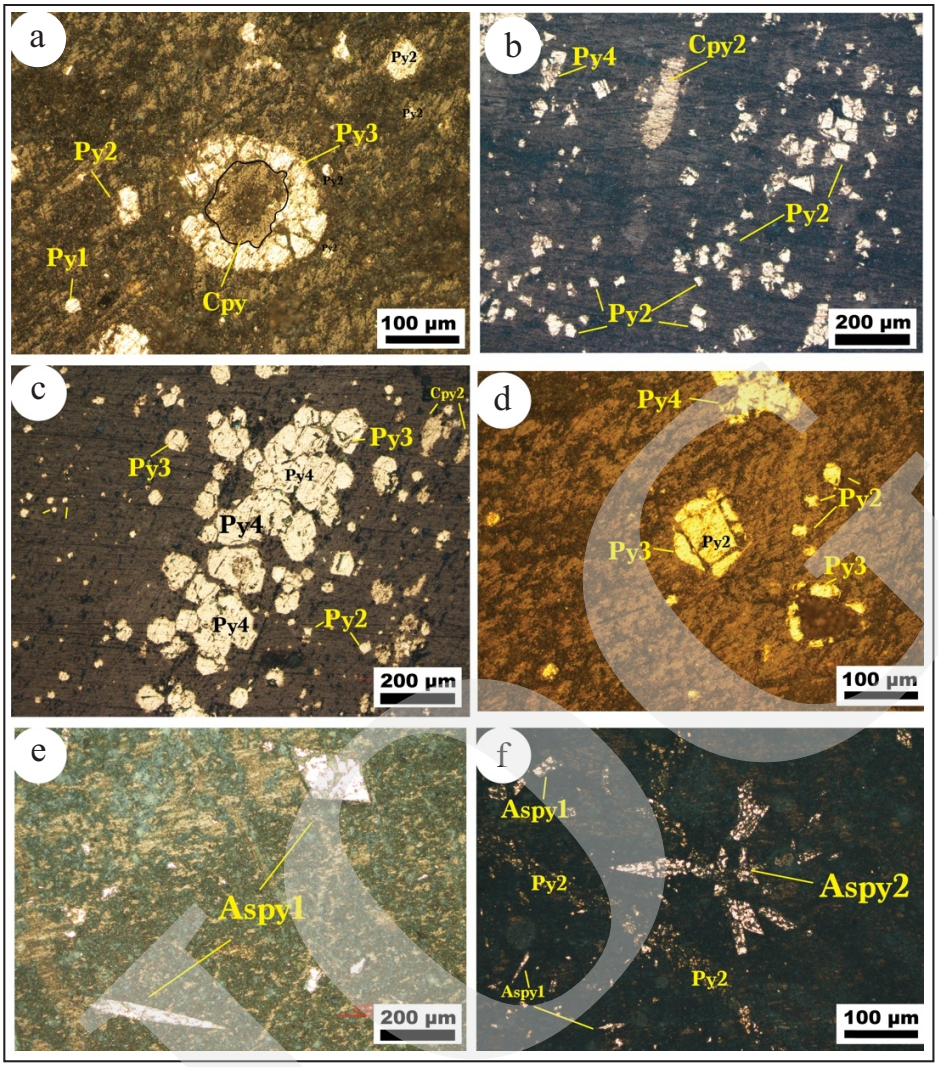

Figure 6. Reflected light photomicrographs display pyrite paragenesis within shale deposit of Pedawan Formation located in Jugan Hill (a) Hydrothermal rim (Py3) around Cpy1 (b - c) Disseminated fine-grained subhedral to anhedral pyrite in black shale and chalcopyrite forming within fractures (Cpy2) (d) Pyrite overgrowth (Py3) on euhedral pyrite (Py2) and the remnants of pyrite overgrowth beside it. (e) Rhombic arsenopyrite (Aspy1) in shale (f) Acicular arsenopyrite in a radial symmetry (Aspy2).

Py3 have decreased slightly than the trace elements content in Py2. Arsenium concentrations and Co/Ni ratio lowered to 2.4 - 1.62, respectively. Post-diagenetic pyrite (Py4) as the last stage of pyrite occurs as aggregates or clusters, and has the lowest Au concentration (50 - 20 ppm). Consistent with the Au concentrations, Arsenium concentrations and Co/Ni have decreased significantly to 80 - 30 ppm and 0.78 - 0.58 ppm, respectively (Table 2; Figure 8).

Fluid Inclusion Petrography

Fluid inclusions are tiny microscopic bubbles containing small quantities of liquid (L), gas (G), or mixtures of both phases, and they are all trapped as impurities within the mineral structure. The fluid inclusion can provide useful information about the minimum trapping temperature. Fluid petrography conducted carbonate samples to characterize the fluid in terms of its genetic classification, types, phase ratios, size, and shape of fluid inclusions. From each side of the section the average of six numbers of inclusions were selected for petrography analysis. The inclusions were classified into quartz and calcite samples. The four types of fluid inclusions are classified as: 1) Type I is aqueous liquid monophase (L_{H2O}), 2) Type II

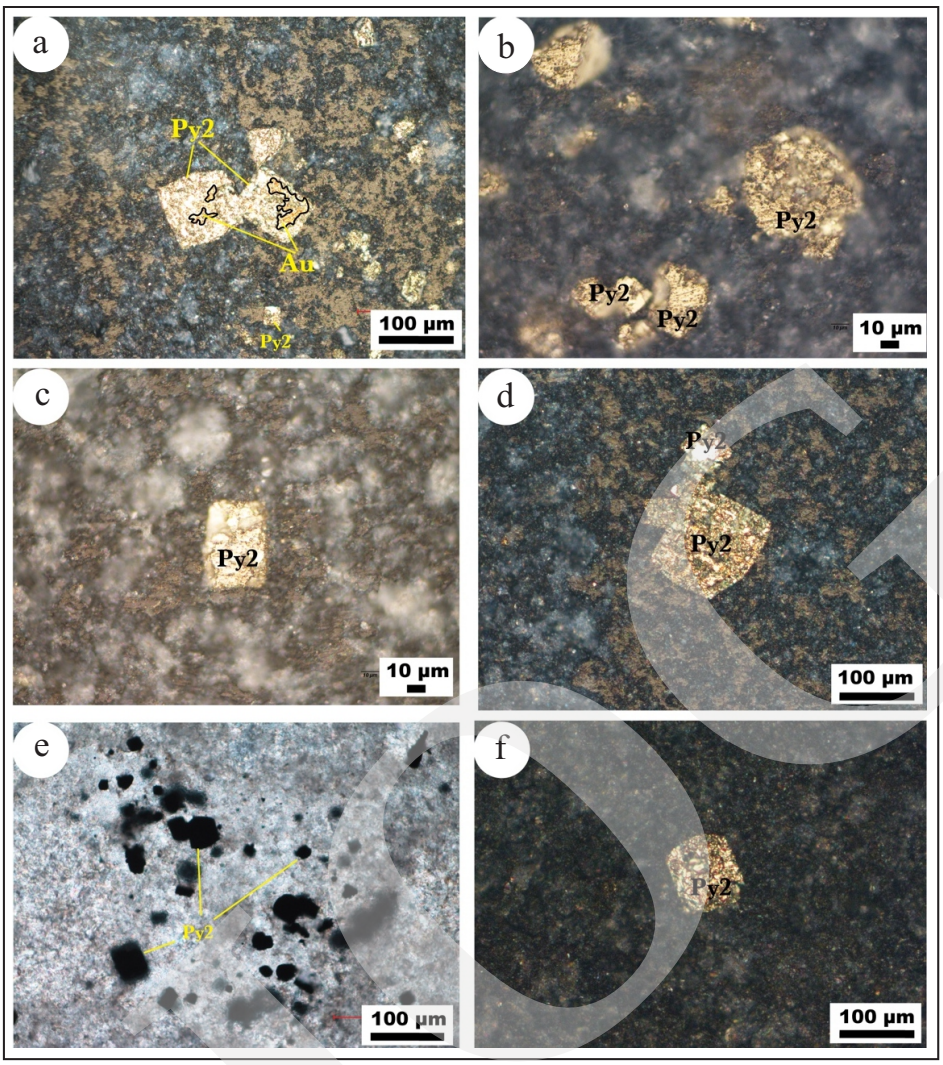

Figure 7. Reflected light and polarized light photomicrographs of Au from Jalan Pejiru. (a) Euhedral pyrite (Py2) with gold inclusion forming within the grains; (b - f) Disseminated subhedral to euhedral fine-grained pyrite (Py2).

Table 2. EPMA Results for Gold and Trace Element Composition of Different Stages of Pyrite

Pyrite stages	Fe (%)	S (%)	Total (%)	Stdev	As (ppm)	Cu (ppm)	Co (ppm)	Au (ppm)	Ni (ppm)	Co/Ni
Py1	45.51	53.1	98.61	5.37	450	20	420	45	750	0.56
	45.24	52.12	97.36	4.86	520	24	550	70	675	0.81
Py2	44.62	52.16	96.78	5.33	650	10.8	830	390	450	1.84
	44.93	52.97	97.9	5.69	570	20	685	282	260	2.63
Py3	45.04	52.19	97.23	5.06	280	24	360	220	150	2.4
	45.19	53.16	98.35	5.64	150	9	130	175	80	1.62
Py4	45.21	53.46	98.67	5.83	80	7	110	50	140	0.78
	45.12	53.02	98.14	5.59	30	5	70	20	120	0.58

is aqueous biphase (L_{H2O}+V_{H2O}), 3) Type III is carbonic monophase phase (L_{CO2}), and 4) Type IV is polyphase inclusion (L_{H2O}+V_{H2O}+solid) in quartz and calcite (Tables 3 and 4; Figure 9).

Discussion

In general, Carlin Au deposit occurs in both visible (native) and invisible (micron-nano) form,

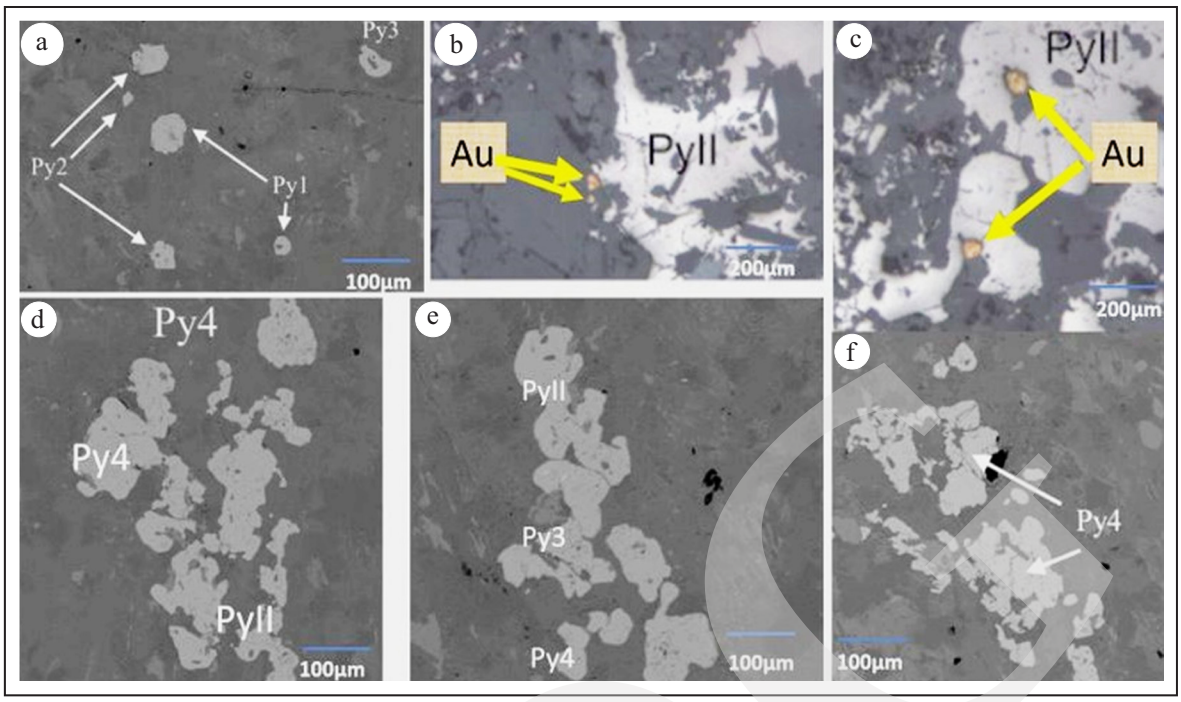

Figure 8. Different stages of pyrite within shale sample from the Jugan Hill. (a) Framboidal, subhedral and zoned pyrite (Py1, Py2 and Py3). (b - c) Native gold inclusion adjacent to Py2. (d) Subhedral to cluster form of pyrite within shale deposit of Jugan Hill (Py2 and Py4). (e) Subhedral, overgrowth and cluster of pyrite (Py2, Py3, and Py4). (f) Pyrite aggregates within shale deposit of Jugan Hill (Py4).

Table3. Petrography of Fluid Inclusions in Calcite Vein

Genetic classification (P/S)	Type	Phases	Size (µm)	Phase ratio (Liquid: Vapor)	Shape
Primary	I	Liquid	8	80:20	Rounded, Irregular
Primary/Secondary	II	Liq.+Vapour	8	100	Rhombic
Primary	III	Vapour	4	100	Rectangle
Primary	IV	Liquid	10	100	Square

Table 4. Petrography of Fluid Inclusions in Quartz Vein

Genetic classification	Type	Phase	Size (µm)	Phase ratio (Liquid: Vapour)	Shape
Primary	I	Liquid	8	80:20	Rounded, Irregular
Primary/Secondary	II	Liq.+Vapour	8	100	Rhombic
Primary	III	Vapour	4	100	Rectangle
Primary	IV	Liquid	10	100	Square

and associated with sulphides (pyrite, arsenian pyrite, and chalcopyrite) in the form of lattice bound or invisible form in Nevada and China (Fleet *et al*., 1993; Arehart, 1996; Petrella *et al*., 2022; Yin *et al.,* 2023; Yu *et al*., 2024). For the Bau deposit, pyrite is the main host for micron-nano size Au, and trace elements were incorporated into different stages of pyrite. The trace elements predominantly occur in different stages of pyrite lattice and micron-nano sized Au, and trace elements occur infilled with microstructure of different stages of pyrite. The alteration like pyritization (fine and disseminated pyrite grains) and silicification (siliceous limestone) are the im-

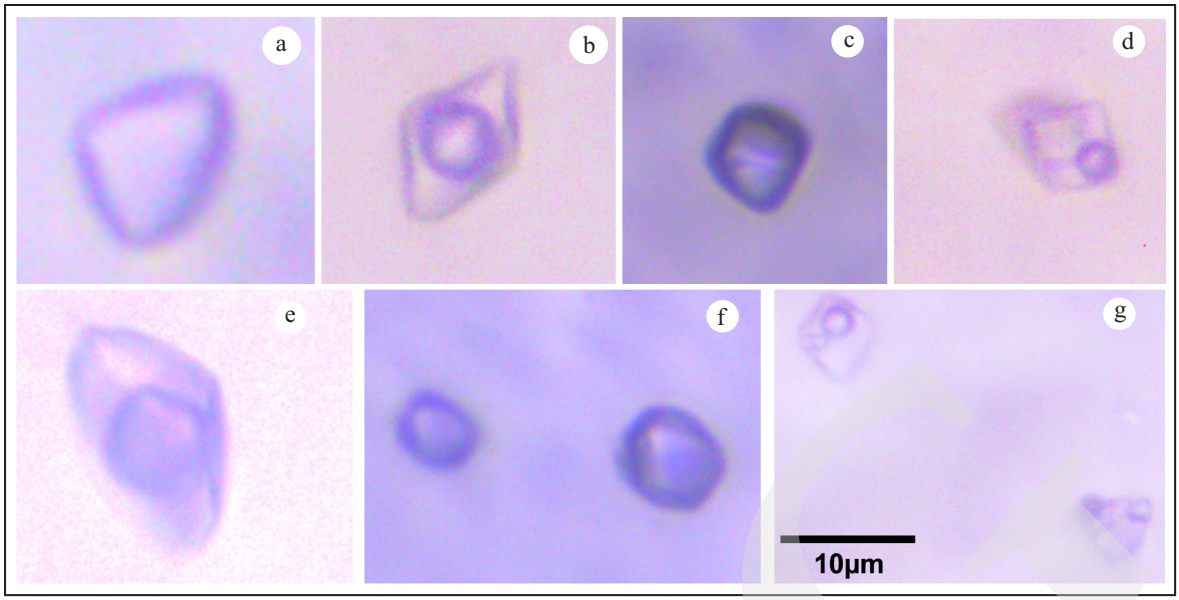

Figure 9. Fluid inclusion in calcite (a - d) and quartz (e - f) vein samples, Bau, Kuching, Sarawak. (a) Aqueous liquid monophase, (b) aqueous biphase liquid rich, (c) Carbonic inclusion, (d) polyphase in calcite, (e) Aqueous biphase inclusion Carbonic phase, (f) Carbonic monophase, (g) Multi-solid inclusion in quartz.

portant features for sediments hosted Au deposit (Zhou and Wang, 2003; Petrella *et al*., 2022; Yin *et al.,* 2023; Yu *et al*., 2024). In the EPMA experiment, the average values of Fe and S values in different stages of pyrite corresponds to 45 - 48 % (Fe) and 54 - 52 % (S), respectively. Co-Ni are important geochemical path finder element pair to know the origin of pyrite. The concentrations of Co, Ni, and Co/Ni ratios are important for Carlin and gold mineralization types (Zhu *et al*., 2011, Large *et al*., 2014; Gregory *et al*., 2015; Yin, 2023). The content of Au increases with the increase concentration of Co and the decrease of Ni contents in different stages of pyrite, because Ni and Co were incorporated into Au for transporting into pyrite lattice providing the information on the gold precipitating mechanism in Bau deposit. The Bau deposit is spatially associated with sedimentary units, and contains relatively moderate concentration of Ni (750 - 120 ppm) and Co (830 - 70 ppm) in different stages of pyrite. The Co/Ni ratio for Py1 (stage 1) is characterized by 0.56 - 0.81, and Py4 (stage 4) is characterized by 0.58 - 0.78 ppm implying the origin of sedimentary pyrite (<1). Whereas Co/Ni ratio in Py2 (stage 2) and Py3 (stage 3) were characterized by continuously crystallizing (increase the Au amount). The variations in the As, Ni, and Co abundant in different stages of pyrite (FeS_2) reflect the fluctuation in the fluid complex (Bralia *et al*., 1979; Cook and Chryssoulis, 1990; Cook, 1996). The main gold precipitation takes place in Py2 and Py3. In this stage, it identified few visible gold grains along with Py2−3 stages. Auriferous pyrite was precipitated from H (aqueous inclusion) and S (reduced condition) rich in the fluid complex, and Au may be trapped in the form of lattice bound $Au(HS)^0$ or $Au(HS)^{2-}$ (Seward, 1990; Hofstra and Cline, 2000; Su *et al*., 2012; Yu *et al*., 2024). So, the H and S rich fluid complex were played an important role for transporting the Au into the pyrite lattice. The above discussions clearly imply Au precipitate in the multiple stages of pyrite lattice.

Conclusion

For Bau Au deposit, some key conclusions are drawn from the ore mineralogy, mineral chemistry, and fluid inclusions. Four stages of pyrites were distinguished: pre-diagenetic disseminated framboidal pyrite (Py1), continued crystallization form Py2 of subhedral to euhedral pyrite,

overgrowth on Py2 formed Py3, and continued growth on Py2 and Py3 precipitates the last generation of pyrite (Py4). Type 2 and Type 3 stages of pyrite as the main Au precipitation stage and incorporated into pyrite lattice. It is regulated by H. S, Co, and Ni rich fluid ligands, and aqueous-carbonic fluids were played a major transporting media for this deposit. Micron-nano size Au and other trace elements were incorporated into different stages of pyrite, and associated with the carbonate rock units of Bau, Kuching. The study of lattice bound Au in different stages of pyrites shows that Py1 was pre-diagenetic stage in origin, whereas Py2 and Py3 were formed during the diagenetic stage, whilst Py4 was formed during post-diagenetic stage. The Au and trace elements were incorporated into different stages of pyrite and substitute of sulphur (S) and iron (Fe) in all stages of pyrite. The Au (Py1) introduced at early diagenetic stage and continually incorporated into different stages. The release of Au and trace elements were infilled and transported by aqueous-carbonic fluids and the fluid ligands. The pyrite texture and mineral chemistry of different stages of pyrite imply multiple stage distribution of micron-nano Au in Bau deposit.

Acknowledgement

This study was financially supported by CMRI-CRS (Grant No. 006043), Curtin University, Malaysia for this research work. The authors are also thankful to the the IJOG Chief and Editors, as well as anonymous reviewers for their constructive comments and suggestions to improve the quality of the manuscript.

References

Ahmed, N., Siddiqu, N.A., Abd Rahman, A.H., Hanif, T., and Kasim, S.A., 2020. Belaga Formation, A Deep Marine Rock Unit of Rajang Group How It Looks Like in The Field, Central Sarawak, North-Western Kalimantan. *Science International (Lahore),* 32 (5), p.521-525.

Arehart, G.B., 1996. Characteristics and origin of sediment-hosted disseminated gold deposits: A review. *Ore Geology Reviews*, 11 (6), p.383-403.

Berger, V.I., Mosier, D.L., Bliss, J.D., and Moring, B.C., 2014. Sediment-hosted gold deposits of the world-Database and grade and tonnage models. *U.S. Geological Survey Open file report,* 2014-1074. p.1-46.

Bralia, A., Subatini, G., and Troja, F., 1097. A Revaluation of the Co/Ni ratio in pyrite as a geochemical tool in ore genesis problems. Evidences from southern tuscany pyritic deposits. *Mineralium Deposita,* 14, p.353-374.

Butler, I.B. and Rickard, D., 2000. Framboidal pyrite formation via the oxidation of iron (II) monosulfide by hydrogen sulphide. *Geochimica et Cosmochimica Acta,* 64, p.2665-2672.

Cabri, L.J., Chryssoulis, S.L., de Villiers, J.P.R., Laflamme, J.H.G., and Buseck, P.R., 1989. The nature of "invisible" gold in arsenopyrite. *Canadian Mineralogist,* 27 (3), p.353-362.

Cook, N.J. and Chryssoulis, S.L., 1990. Concentrations of "Invisible Gold" in the common sulfides. *Canadian Mineralogist,* 28, p.1-16.

Cook, N.J., 1996. Mineralogy of the sulphide deposits at Sulitjelma, northern Norway. Ore Geology Reviews, 11(5), p.303-338

Farrand, M., 1970. Framboidal sulphides precipitated synthetically. *Mineralium Deposita,* 5, p.237-247.

Galin, T., Breitfeld, H.T., Hall, R., and Sevastjanova, I., 2017. Provenance of the Cretaceous-Eocene Rajang Group submarine fan, Sarawak, Malaysia from light and heavy mineral assemblages and U-Pb zircon geochronology. *Gondwana Research,* 51, p.209-233.

Goldfarb, R.J., 2021. Lode Gold Deposits in Time and Space. *Encyclopedia of Geology (Second Edition),* p.663-679.

Gregory, D.D., Large, R.R., Halpin, J.A., Baturina, E.L., Lyons, T.W., Wu, S., Danyushevsky, L., Sack, P.J., Chappaz, A., Maslennikov, V.V., and Bull, S.W., 2015. Trace element content of

sedimentary pyrite in black shales. *Economic Geology*, 110 (6), p.1389-1410.

Hofstra, A.H. and Cline, J.S., 2000. Characteristic and models for Carlin-type gold deposits. *Reviews in Economic Geology*, 13, p.163-200.

Hon, V., 1981. Physical controls of mineralization in the Bau Town area, west Sarawak, Malaysia. *Sarawak Mineralogy Bulletin,* 1, p.43-45.

Hutchison, C.S., 2005. *Geology of north-west Borneo: Sarawak, Brunei, and Sabah.* Amsterdam: 1st edition Elsevier Science, p.1-444.

Katz, L.R., Kontak, D.J., Dubé, B., McNicoll, V., Creaser, R., and Petrus, J.A., 2021. An Archean Porphyry-Type Gold Deposit: The Côté Gold Au(-Cu) Deposit, Swayze Greenstone Belt, Superior Province, Ontario, Canada. *Economic Geology,* 116 (1), p.47-89.

Kirwin, D.J. and Royle, D.Z., 2018. Sediment-Hosted Gold Deposits in Southeast Asia. *Resource Geology,* 69 (2), p.1-23.

Lambiase, J.J., Tzong, T.Y., William, A.G., Bidgood, M., Brenac, P., and Cullen, A., 2008. The West Crocker formation of northwest Kalimantan: A Paleogene accretionary prism. *Special Paper of the Geological Society of America,* 436, p.171-184.

Large, R.R., Halpin, J.A., Danyushevsky, L.V., Maslennikov, V.V., Bull, S.W., Long, J.A., Gregory, D.D., Lounejeva, E., Lyons, T.W., Sack, P.J., and McGoldrick, P.J., 2014. Trace element content of sedimentary pyrite as a new proxy for deep-time ocean–atmosphere evolution. *Earth and Planetary Science Letters*, 389, p.209-220.

Large, R.R. and Maslennikov, V.V., 2020. Invisible Gold Paragenesis and Geochemistry in Pyrite from Orogenic and Sediment-Hosted Gold Deposits. *Minerals,* 10 (4), p.339.

Macdonald, E.H., 2007. *Handbook of gold exploration and evaluation*. Woodhead Publishing Limited, 647pp.

Morishita, Y., Shimada, N., and Shimada, K., 2018. Invisible gold in arsenian pyrite from the high-grade Hishikari gold deposit, Japan. Significance of variation and distribution of Au/Ag ratios in pyrite. *Ore Geology Reviews,* 95, p.79-93.

Moss, S. and Chambers, J.L.C., 1999. Tertiary facies architecture in the Kutai Basin, Kalimantan, Indonesia. *Journal of Asian Earth Sciences,* 17 (1), p.157-181.

Muller, J., 1968. Palynology of the Pedawan and Plateau Sandstone Formations (Cretaceous-Eocene) in Sarawak, Malaysia. *Micropaleontology*, 14 (1), p.1-37.

Muntean, J.L., Cline, J.S., Simon, A.C., and Longo, A.A., 2011. Magmatic-hydrothermal origin of Nevada's Carlin-type gold deposits. *Nature Geoscience,* 4, p.122-127.

Mustard, H., 1997. The Bau Gold district, Aus-IMM. *World Gold Conference '97*, Singapore. p.21.

Percival, T.J., Radtke, A.S., and Bagby, W.C, 1990. Relationships Among Carbonate-Replacement Gold Deposits, Gold Skarns, and Intrusive Rocks, Bau Mining District, Sarawak, Malaysia. *Mining Geology,* 40 (1), p.1-16.

Percival, T.J. and Hofstra, A.H., 2002. Bau, Malaysia: SRHDC deposit associated with Miocene magmatism. *Geological Society of America,* 34, p.142.

Petrella, L., Thébaud, N., Fougerouse, D., Tattitch, B., Martin, L., Turner, S., Suvorova, A., and Gain, S., 2022. Nanoparticle suspensions from carbon-rich fluid make high-grade gold deposits. *Nature Communications,* 13, p.3795.

Pour, A.B., Hashim, M., and Marghany, M. 2014. Exploration of gold mineralization in a tropical region using Earth Observing-1 (EO1) and JERS-1 SAR data: a case study from Bau gold field, Sarawak, Malaysia. *Arabian Journal of Geosciences,* 7, p.2393-2406.

Royle, D.Z., 2015. Characteristics of sediment-hosted epithermal deposits. World class ore deposits: Discovery to recovery. Society of Economic Geologists-CODES Conference, Hobart, Australia (abstract and poster), P009.

Schuh, W.D., 1993. *Geology, geochemistry, and ore deposits of the Bau gold mining district, Sarawak, Malaysia.* Doctoral Dissertation,

The University of Arizona. https://repository.arizona.edu/handle/10150/187561.

Seward, T.M., 1990. The hydrothermal geochemistry of gold. *In*: Foster. R.P. (ed.), *Gold Metallogeny and Exploration*, p.37-62. Spinger Nature.

Sillitoe, R.H. and Bonham, H.F., 1990. Sediment-hosted gold deposits: Distal products of magmatic-hydrothermal systems. *Geology,* 18 (2), p.157-161.

Su, W., Zhang, H., Hu, R., Ge, X., Xia, B., Chen, Y., and Zhu, C., 2012. Mineralogy and geochemistry of gold-bearing arsenian pyrite from the Shuiyindong Carlin-type gold deposit, Guizhou, China: implications for gold depositional processes. Mineralium Deposita, 47, p.653-662.

Syafiq, H., Shah, A.A., and Rachman, M.G., 2024.Shuttle radar topography-based analysis reveals the active Borneo Island Fault in Borneo, SE Asia. *Journal of Asian Earth Sciences*, 12, 100184.

Tan, D.N., 1986. Paleogeographic development of west Sarawak. *GEOSEA V, Proceedings,* 1 (19), p.39-49.

Tate, R.B., 1991. Cross-border correlation of geological formation in Sarawak and Kalimantan. *Geological Society of Malaysia,* 28, p.63-95.

Wang, P.C., Li, S.Z., Guo, L.L., Jiang, S.H., Somerville, I.D., Zhao, S.J., Zhu, B.D., Chen, J., Dai, L.M., Suo, Y.H., and Han, B., 2016. Mesozoic and Cenozoic accretionary orogenic processes in Kalimantan and their mechanisms. *Geological Journal*, 51, p.464-489.

Wilford, G.E., 1955. The geology and mineral resources of the Kuching-Lundu area, West Sarawak, Including the Bau Mining District. *Geologycal Survey of Borneo, Memoir*, 3, 254pp.

Wolfenden, E.D., 1965. Bau mining district, West Sarawak. Malaysia, Bau Geologycal Survey Borneo Region. *Malaysia, Bulletin,* 7, p.1-147.

Yao, B., 1999. The Geotectonic Character of SE Asia and Cenozoic Tectonic History of South China Sea. *Guangzhou Marine Geological Survey,* 2 (4), p.512-515.

Yin, J., Sun, Y., Yin, H., Shi, H., Sparling, J., Chao, Y., and Xiang, S., 2023. Correlations between trace elements in pyrite and gold mineralization of gold deposits on the North China platform. *Acta Geochimica*, 42 (6), p.1079-1103. DOI: 10.1007/s11631-023-00636-4

Yu, H.D., Yu, L.M., Said, N., Huang, C.C., Wu, J.H., Liu, C.M., Chen, H.F., and Zou, H., 2024. The Paleo-Tethys subduction and related mineralization in the SW Yangtze Block: Evidence from the Zhesang Carlin-type gold deposit. *Geosystems and Geoenvironment*, 3 (2), p.100086.

Zhou, Y.J. and Wang, 2003. Gold in the Jinya Carlin-type deposit: characterization and implications. *Journal of Minerals and Materials Characterization and Engineering*, 2 (02), p.83.

Zhu, Y., An, F., and Tan, J., 2011. Geochemistry of hydrothermal gold deposits: A review. *Geoscience Frontiers,* 2 (3), p.367-374.